Flow rheology of light foams generated from aqueous solutions of polyvinyl alcohol

ARI JÄSBERG, JANIKA VIITALA, ATSUSHI TANAKA, BARANIVIGNESH PRAKASH, AND ANTTI I. KOPONEN

ABSTRACT: Recent studies have shown that foam-assisted application of additives into a wet web has advantages over the conventional way of adding the chemicals into the pulp suspension before forming, e.g., increased mechanical retention as well as high dosage giving increased wet strength without impairing the sheet uniformity. To engineer processes utilizing this new technology, the complex flow behavior of applied foams must be quantified. At the minimum, the foam viscosity and the slip velocity at the solid surfaces need to be known to build practical models that can be used in analyzing and upscaling unit processes of the foam-assisted application.

In this study, the rheological behavior was quantified for foams having polyvinyl alcohol (PVOH), a widely used strength additive chemical, as the surfactant. The foam density was varied between 100 g/L and 300 g/L, and the concentration of the PVOH solution was varied between 0.5% and 6.0% (w/w). The foams were generated with a commercial foam generator, and the rheological properties of the foams were measured by using a horizontal pipe bank. At the outlet from the generator, the volumetric flow rate, the absolute pressure, and the bubble size distribution of the foam were measured. In the measurement pipe section, the viscous pressure gradient and the slip velocity were measured, after which the foam was discharged to ambient air pressure. The viscosity and the dynamic surface tension of the PVOH solutions were quantified with commercial laboratory devices.

In the viscosity analysis, the apparent shear rate was calculated from the volumetric flow rate, and the resulting apparent viscosity was translated to real material viscosity data by applying the Weissenberg-Rabinowitsch correction. The results indicated that PVOH foams can be described with high accuracy as shear-thinning power-law fluids where the detailed behavior depends on the foam density and the PVOH concentration. Slip flow, as usual, increased with increasing wall shear stress, but it was also dependent on the PVOH concentration, the air content, and the bubble size. For both the foam viscosity and the slip flow, a correlation was found that described the quantitative behavior of all the studied foams with good accuracy.

Application: This study helps engineers to develop foam coating devices and processes by providing rheological correlations for foam viscosity and slip flow.

In the foam-assisted application process, foam is used as the carrier phase of the applied materials, i.e., chemical solutions or particle dispersions. While foam coating is an established technology in the textile industry [1,2], the utilization of foam application in the paper and board industry is still in its infancy. Foam application to the wet web, however, would offer advantages over the conventional way of dosing the chemicals to the fiber stock before forming [3-8]. In the conventional process, strength additives may increase fiber flocculation, especially with high dosage levels, and the applied chemicals need to have a high adsorbing tendency on the fiber surfaces; otherwise, they may end up in water circulation instead of the final product. Foam application allows dealing with high viscosity solutions and has high mechanical retention, and one can control the penetration depth of the applied material to the porous substance. A close cousin of foam application, spray application, has its problems, such as the creation of mist, the difficulty of dealing with highly viscous fluids limiting the dosage levels of chemicals, the high clogging tendency of the spray nozzles, and problems in obtaining uniform coverage of the base with the sprayed chemical. Finally, notice that in papermaking, foam application could also be used for improving the dryness of the web after pressing [5,9].-

Foams consist of three components that are mixed in a foam generator: water, air, and surfactant. The air content of the application foam is typically between 80% to 95% (v/v), and the bubble size is of the order of 100 µm. In addition to the air content and the bubble size, the rheology of the foam is affected by the viscosity and the surface tension of the base solution (water + surfactant). The rheological bulk behavior of foam is usually well represented by the Herschel-Bulkley equation [10,11]:

$$\tau = \tau_0 + K\dot{\gamma}^n \quad (1)$$

where τ is shear stress, τ_0 is yield stress, $\dot{\gamma}$ is shear rate, K is

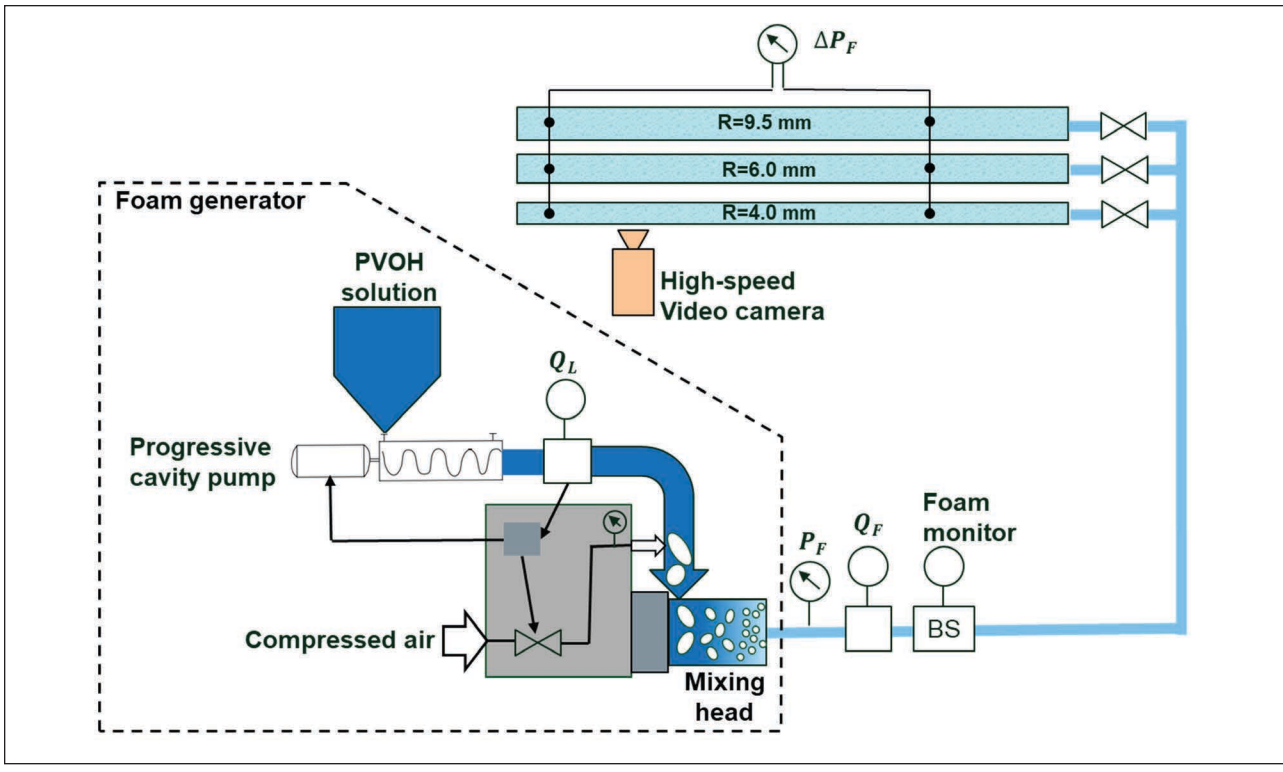

1. Schematic drawing of the components in the experimental setup. The foam generator used for establishing the flow is shown inside the dashed polygon, and the components outside the polygon are the flow line and measurements used for quantifying the flow rheology of foam. The setup contains the measurements for the volumetric flow rate Q_L of the liquid surfactant solution (an integral part of the foam generator), absolute back pressure P_F at the foam generator outlet, the volumetric flow rate Q_F of the foam, the bubble size distribution (BS) of the foam, and the pressure drop ΔP_F in the foam flow over a fixed span of the test pipe section (0.3 m span for the R = 4.0 mm pipe, and 1.0 m span for the other two pipes).

the consistency index, and n is flow index. Yield stress is often omitted from Eq. 1, as it is typically small compared to applied stress. One can then alternatively write:

$$\mu = K\dot{\gamma}^{n-1} \quad (2)$$

where μ is the foam viscosity. Notice that at the solid walls, foams have a strong tendency for slip flow, the magnitude of which depends on the foam properties and the shear stress at the wall [12-14].

In this work, we performed a systematic study on foam rheology. Due to problems related to the aging of foam and slip flow, rheological analysis of foams is not feasible with most traditional rheometer geometries, and we used pipe flow for this purpose. We varied air content, surfactant dosage, and flow rate in a wide range; the final number of trial points exceeded 300. As the surfactant, we used polyvinyl alcohol (PVOH), as it is widely used by the paper and paperboard industry as a strength additive.

MATERIALS AND METHODS

Experimental setup

The rheological parameters for foams generated by using polyvinyl alcohol (PVOH) as a surfactant were quantified in a laboratory-scale pipe flow test environment shown in **Fig. 1**. Foam flow was established with a foam mixer manufactured by Hansa Industrie-Mixer GmbH & Co. KG (Stuhr, Germany), as shown in **Fig. 2a**. In Fig. 1, the mixer is shown inside the dashed polygon, and it consists of two subunits: a pumping station for enforcing a constant volumetric flow rate Q_L of the liquid surfactant solution, and a foaming station. In the foaming station, a well-controlled amount of compressed air is added to the liquid and dispersed into small bubbles, thereby generating foam. Based on the mass flow rate set by the user (the user sets the liquid density as well) and the absolute pressure measured at the point of air addition, the device adjusts the air flow so that the density of foam discharging to standard conditions (absolute pressure 1 atm, temperature 20°C) at the end of the flow line stays constant. Breaking air into small bubbles takes place in a mixing head, the so-called rotor-stator assembly, which is shown in Fig. 2b with the stationary stator element detached. Both the stator and rotor have a matrix of protruding pins. The pin rows of the revolving rotor slide in the gaps between the pin rows of the stator. While the mixture of surfactant solution and air flows through the mixing head (main flow direction being axial and out from the mixer), a dynamic high-shear flow field in the gaps between the pin rows breaks air into bubbles. The foam mixer is operated by setting the target values for the rotating

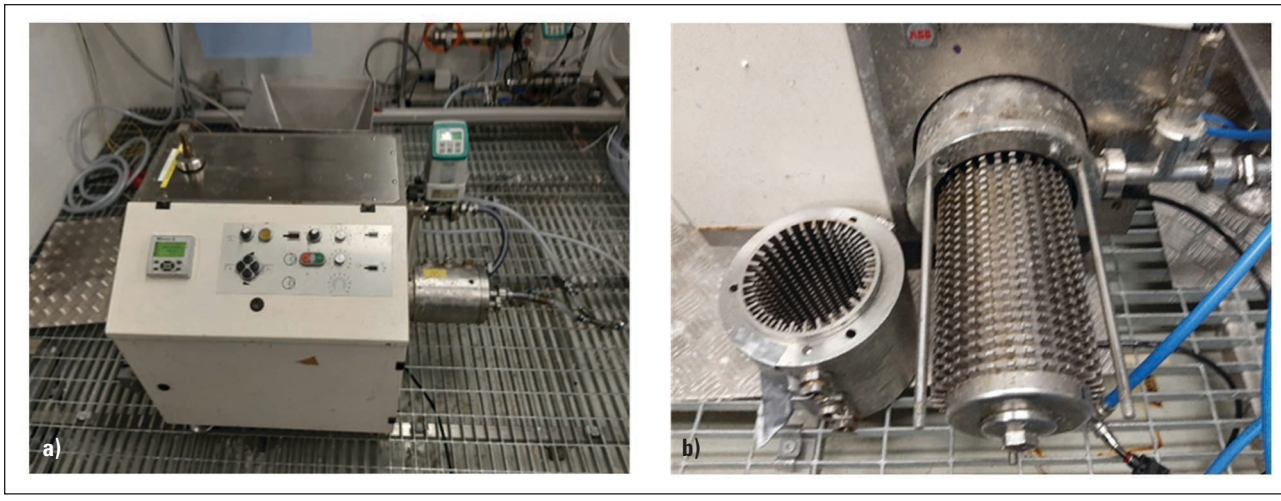

2. a) The foam generator used in the study, and b) the mixing head unit (rotor-stator) opened.

speed of the rotor element, the mass flow rate, and the foam density.

At the outlet from the generator, the volumetric flow rate Q_F, absolute back pressure P_F, and bubble size distribution of foam were measured with a magnetic flow meter, pressure sensor, and an online foam monitoring device [15], respectively. After the online measurement section, foam flowed into a horizontal pipe bank with three parallel 1.5-m-long acrylic pipes with inner radii R = 4.0, 6.0, and 9.5 mm. One pipe at a time was chosen by operating manual valves at the pipe inlets. The foam flow in the pipe was always laminar with the used flow rates. The viscous pressure drop was measured over a fixed span of pipe, after which the flow discharged to ambient room air pressure. The span was 0.3 m for the smallest 4.0 mm pipe, and 1.0 m for the other two pipes.

It is well known that foam flow in a pipe may violate the so-called no-slip boundary condition, which holds for most one-phase continuum fluids. This condition states that the flow velocity of a fluid at a solid wall of a pipe matches the velocity of the wall. In foam flow, the interactions at the pipe wall cause a thin layer of liquid without air bubbles to develop at the wall, and foam bubbles slide on top of this slip layer. A plausible explanation for the formation of the slip layer is that the shear forces near the pipe wall drag out liquid from the nearby regions between the bubbles, especially plateau borders, to the wall [16,17]. Wall slippage can be reduced or prevented by roughening or profiling the walls [18]. In rheometry, for example, a typical way to kill slip is to attach sandpaper to the inner walls of the measurement geometry. Acrylic pipes are typically very smooth (surface roughness 15 µm or below) and known to create large slip velocities, whereas galvanized iron pipes, for example, have a surface roughness of 150 µm or more, and thus foam may flow in those pipes without slipping [16].

The velocity difference between the pipe wall and the foam flow is called slip velocity. Usually, the slip layer is only a few microns thick, i.e., it is very thin as compared with the mean bubble diameter or with the pipe radius. Thus, in the analysis, one can consider foam filling the pipe fully, and the slip velocity is considered as a non-zero velocity boundary condition at the pipe wall. In this work, the slip velocity was quantified by recording the foam motion in the vicinity of the pipe wall with a high-speed video camera. Notice that the mean bubble size was defined as the volume-weighted average (volume moment mean diameter):

$$D_{43} = \frac{\sum_i n_i D_i^4}{\sum_i n_i D_i^3} \quad (3)$$

Materials

The Kuraray Poval 6-88 (Kuraray Poval; Frankfurt, Germany) PVOH was used as a surfactant in this study [19]. It has low molecular weight and a degree of hydrolysis in the range of 86.7–88.7. The measurements were carried out with solutions prepared by cooking PVOH with tap water at a 10% concentration and diluting the cooled solution to measurement concentrations of 0.5%, 1.0%, 3.0%, and 6.0% by weight; the concentration of each diluted batch was verified in the laboratory. The cooking was initiated by heating 100 L of water to the temperature of 50°C and gradually adding solid PVOH resin into the water. Next, the temperature was raised to 85°C, and cooking was continued until the turbidity of the solution disappeared (a few hours). All PVOH solutions were prepared from the same delivered batch of solid resin, and they were stored at room temperature for no more than a few days before being used in the experiment.

Foam pipe flow measurements were carried out with initial PVOH solution in thermal equilibrium with room temperature of ~20°C, and foam density was varied between 100 g/L and 300 g/L with 50 g/L increments. For

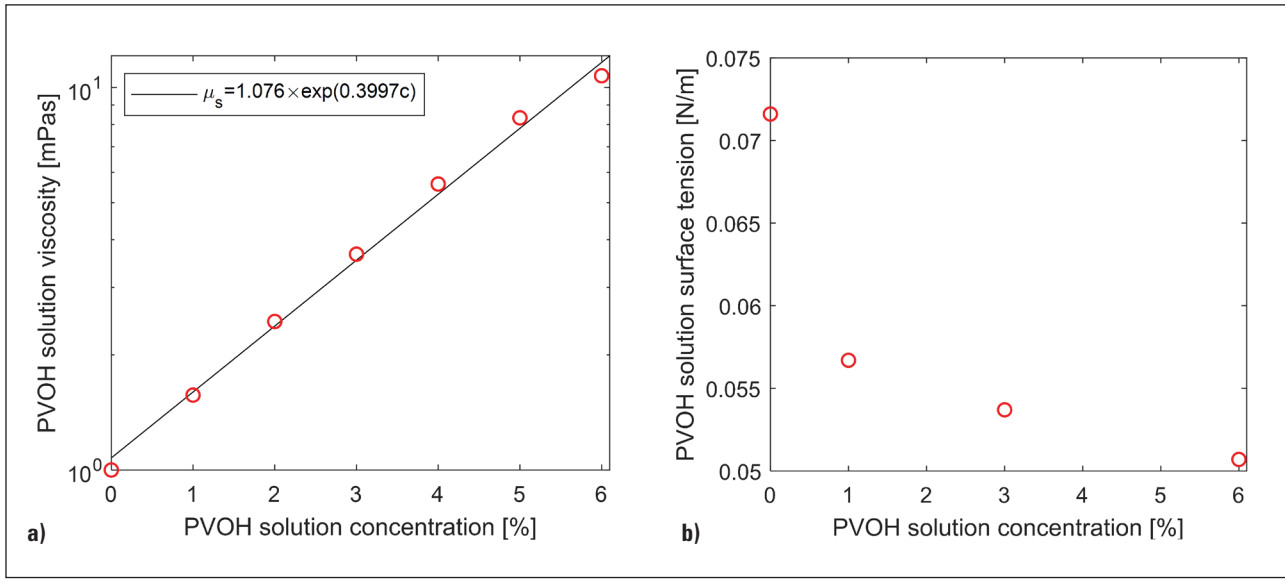

3. a) Polyvinyl alcohol (PVOH) solution viscosity as a function of PVOH concentration. The black line is a fit of the function y = a exp(bx) to the data points. The fit function gives, for 0.5% concentration, the viscosity of 1.3 mPas. b) Measured PVOH solution dynamic surface tension at t = 0.4 s as a function of PVOH concentration. Linear interpolation between 0% and 1% gives, for 0.5% concentration, the surface tension of 0.064 N/m. Surface tension values of 1% and 3% are similar to those obtained with the drop weight method [20].

modeling purposes, the PVOH solution viscosity (**Fig. 3a**) was measured with a Brookfield DV-II+ Pro viscometer (AMETEK Brookfield; Middleborough, MA, USA), and the dynamic surface tension (Fig. 3b) was measured with a KSV Instruments BPA-800P bubble pressure tensiometer (Biolin Scientific; Gothenburg, Sweden).

Notice that PVOH is used in the paper and board industry as a strength additive (glue). So, the PVOH foams studied here could be used as such in real-life processes. If other additives are applied, another surfactant, such as sodium dodecyl sulfate (SDS) might be preferable, as PVOH could affect the performance of the additives.

Converting measured data into viscosity data

In a steady flow in a circular pipe, the wall shear stress is independent of the detailed flow profile and can be calculated from the measured pressure drop per unit length:

$$\tau_w = \frac{R}{2}\frac{dP}{dL} \quad (4)$$

Above, R is the inner radius of the pipe, and dP is the measured pressure drop over the span dL of the flow pipe. To extract material parameters, one must examine the foam in the frame of reference, moving at the speed of the slip velocity. To that end, the slip velocity is subtracted from the average flow velocity:

$$\tilde{v}_{\text{bulk}} = v_{\text{avg}} - v_s \quad (5)$$

Above, v_{avg} is the average flow velocity calculated from the measured volumetric flow rate, v_s is the slip velocity of foam bubbles quantified with the high-speed video camera, and $\tilde{v}_{\text{bulk}}$ is the share of the average flow velocity due to shearing inside the foam plug solely.

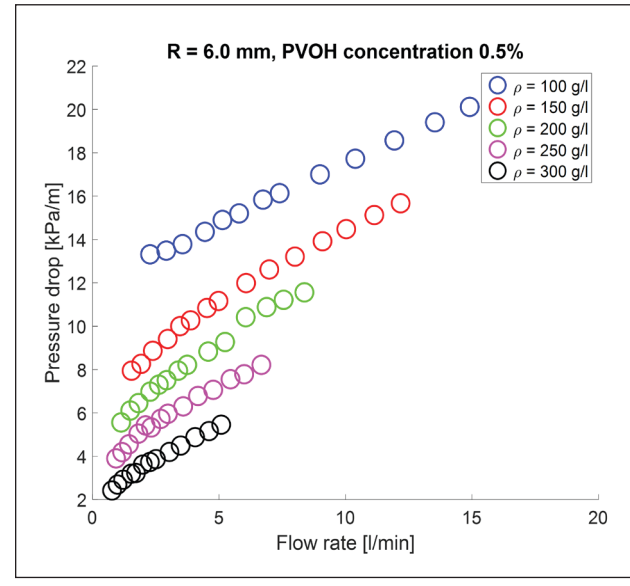

4. Loss curves measured for varying foam density ρ in R = 6.0 mm pipe at 0.5% PVOH concentration.

Apparent foam shear rate $\dot{\gamma}_a$ at the edge of the foam plug is defined as:

$$\dot{\gamma}_a = \frac{4\tilde{v}_{\text{bulk}}}{R} \quad (6)$$

The real shear rate $\dot{\gamma}$ at the pipe wall can now be obtained by applying the Weissenberg-Rabinowitsch correc-

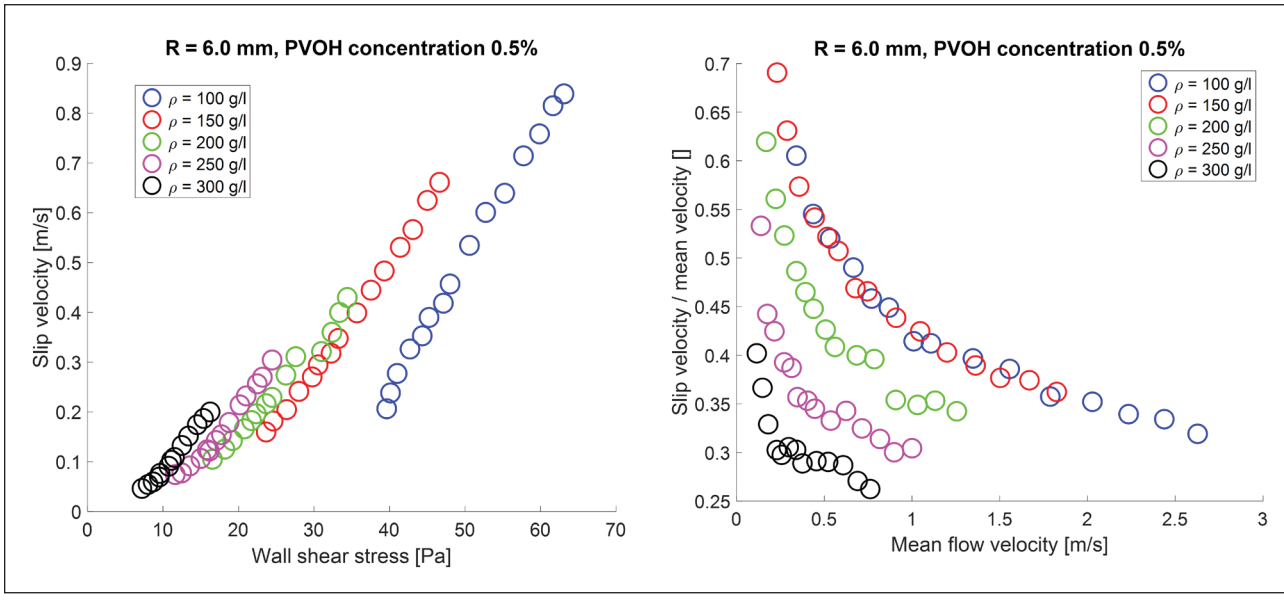

5. Slip velocity data for varying foam density ρ in* R *= 6.0 mm pipe at 0.5% PVOH concentration: a) slip velocity vs. wall shear stress, and b) relative slip velocity vs. mean flow velocity.

tion that considers the non-Newtonian features of the velocity profile [21,22]:

$$\dot{\gamma} = \dot{\gamma}_a \times \frac{1}{4}\left(3 + \frac{d\ln\dot{\gamma}_a}{d\ln\tau_w}\right) \quad (7)$$

Viscosity at a given shear rate is now obtained as the ratio of the wall shear stress to the real wall shear rate:

$$\mu = \tau_w/\dot{\gamma} \quad (8)$$

RESULTS

Examples of measurement data

The total number of trial points was 308. The following three figures show examples of the measurement data for a selected set of process parameters measured in R = 6.0 mm pipe at 0.5% concentration of the starting surfactant solution. Foam density varied between 100 g/L and 300 g/L. **Figure 4** presents the conventional loss curves, i.e., pressure drop per unit length of the pipe vs. volumetric flow rate of foam. The viscous loss increases with decreasing foam density (increasing air content).

Figure 5 shows the slip velocity data. We see from Fig. 5 how the slip correlates with the wall shear stress. In addition, the slip increases with increasing foam density, i.e., an increasing amount of liquid between the bubbles. Figure 5b reveals that the share of the total flow velocity (flow rate) due to slip velocity is highest at low flow rates and decreases with increasing flow rates. At very low flow rates, up to 70% of the measured flow rate was due to slip velocity.

By applying Eqs. 4–8 to the measurement data shown in Fig. 4 and Fig. 5, we end up with the viscosity data plotted in **Fig. 6**. The plotted values are real material parameters without any reference to the used measurements setup (e.g., pipe size). The calculated viscosity values follow the fact that foams are generally power law fluids; their viscosity is, i.e., given with good accuracy by Eq. 2.

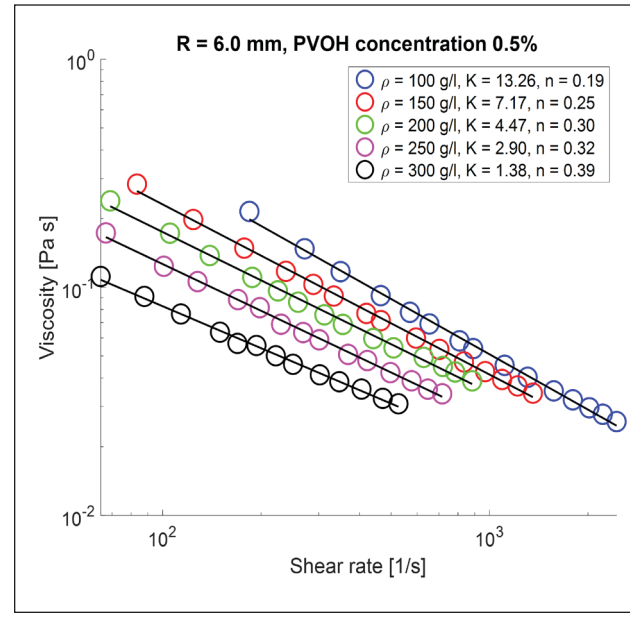

6. Analyzed viscosity for varying foam density ρ in* R*=6.0 mm pipe at 0.5% PVOH concentration. Straight lines are fits of the power law Eq. 2. The fitting parameters* K *and* n *are shown in the legend.

Data analysis

Foams are characterized uniquely by four quantities: air content φ, solution viscosity μ_s, solution surface tension σ; and bubble size D. Air content is obtained from the formula:

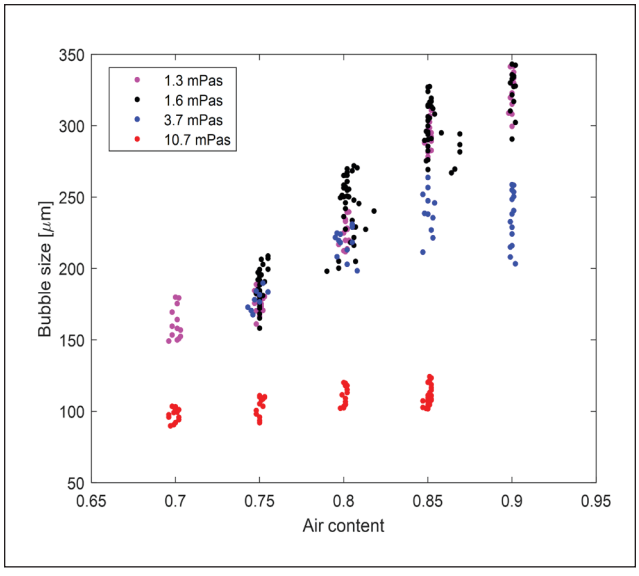

7. Bubble size as a function of air content. The PVOH solution viscosity is shown with different marker colors (note that viscosity is expressed in the legend in mPas). All the trial points are included in the figure.

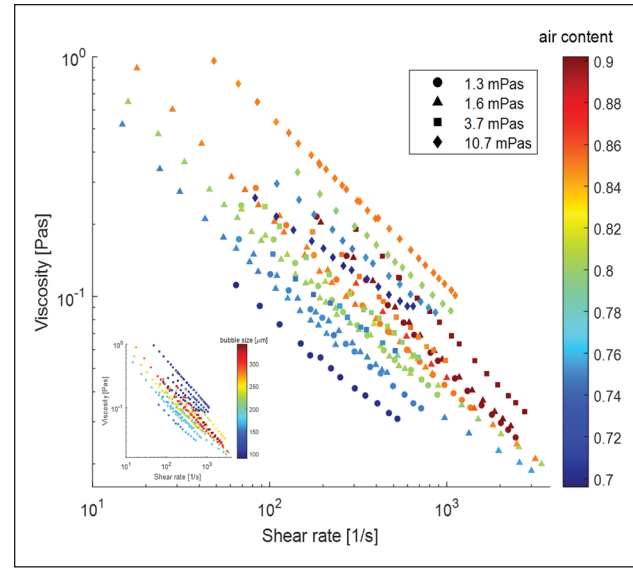

8. Measured foam viscosity as a function of shear rate. The air content is shown with colors, and the viscosity of the PVOH solution is shown with the marker type (note that viscosity is expressed in the legend in mPas). The inset figure shows the bubble size with colors.

$$\varphi = \frac{\rho_s - \rho_f}{\rho_s} \tag{9}$$

where ρ_s is the solution density and ρ_f is the foam density. During the modeling of the two rheological quantities, foam viscosity and slip flow, it turned out that the inclusion of surface tension did not improve the obtained models. Surface tension was thus dropped from the subsequent analysis. **Figure 7** shows the other three quantities for all the trial points. We see that some of the quantities are correlated. Bubble size tends to decrease both with increasing PVOH solution viscosity ($R^2 = 0.78$) and with decreasing air content ($R^2 = 0.61$). Higher solution viscosity likely leads to higher shear forces in the foam generation unit, and bubble size becomes smaller. On the other hand, with higher air content, one would probably need longer processing time and/or higher mixing speed for breaking the bubbles to obtain as small of bubbles as were obtained with the lower air contents. This is substantiated by the fact that bubble size typically increased with the increasing volumetric flow rate of the foam. The collinearity between the bubble size, air content, and solution viscosity must be considered when using them as independent variables in the viscosity and slip flow models.

Analysis of viscosity data

Figure 8 shows the entire measured viscosity data as a function of the shear rate. The air content is shown with colors, and the viscosity of the PVOH solution is shown with the marker type. The inset figure shows the bubble size with colors. We see from Fig. 8 that the relation between the foam viscosity and the shear rate is, as expected, a power law, Eq. 2, in the whole data set. We also see that the foam viscosity generally increases with increasing air content and increasing PVOH solution viscosity. On the other hand, there is no obvious relationship between the foam viscosity and the bubble size.

Assuming power law behavior, Eq. 2, a general model for the foam viscosity can be written as:

$$\mu = K(\varphi, \mu_s, D)\dot{\gamma}^{n(\varphi,\mu_s,D)-1} \tag{10}$$

where φ is air content, μ_s is the viscosity of the PVOH solution, and D is the bubble diameter. Suitable functional forms were found for $K = K(\varphi, \mu_s, D)$ and $n = n(\varphi, \mu_s, D)$ as follows: first, a power law was fitted separately for the $(\dot{\gamma}, \mu)$ –data of each unique flow series (i.e., D, μ_s and φ were fixed; for examples, see Fig. 6). Then, the obtained data sets for K and n were studied separately. It was found that the bubble size had a negligible effect in both cases, and the effect of the solution viscosity was marginal for n. The bubble size apparently had a marginal effect on the foam viscosity, as it was not an independent variable. As we see in Fig. 7, bubble size depended both on the PVOH concentration and the air content, and their effect on the foam viscosity was higher than that of the bubble size.

For both K and n, a power law model was found to work well, i.e.:

$$K = a\varphi^b\mu_s^c \tag{11}$$

and

$$n = d\varphi^e \tag{12}$$

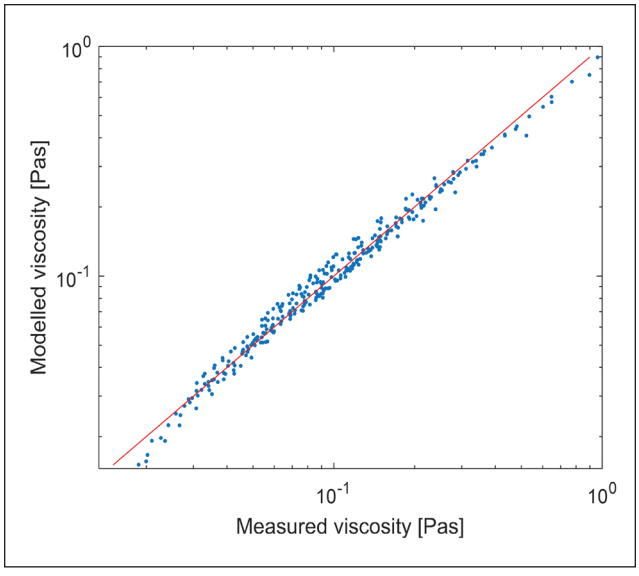

9. The modeled viscosity, Eq. 13, with the parameters shown in Eq. 14 as a function of the measured viscosity. The red line shows the curve y = x. Coefficient of determination is R^2 = 0.99.

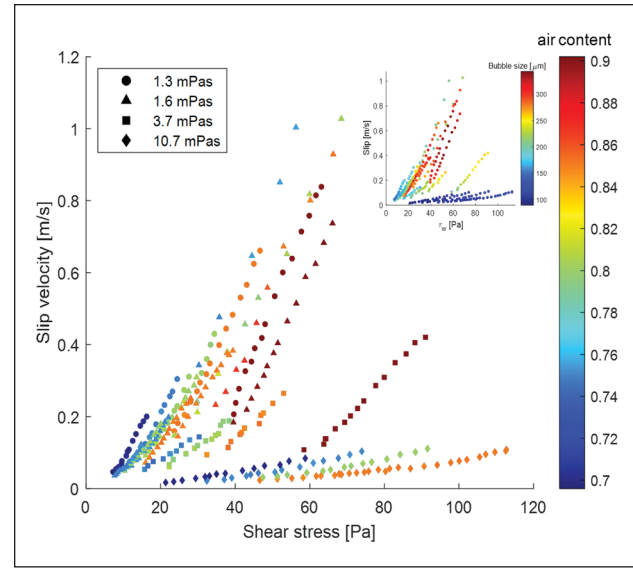

10. The entire data set used for the slip flow analysis. The air content is shown with colors, and the viscosity of the PVOH solution is shown with the marker type. The inset figure shows the bubble size with colors.

(In the preceding, *a*, *b*, *c*, *d*, and *e* were model parameters.) The final model for foam viscosity was then:

$$\mu = a\varphi^b \mu_s^c \dot{\gamma}^{d\varphi^e - 1} \quad (13)$$

(Notice that in Eq. 13, PVOH solution viscosity, μ_s, was expressed in mPas and shear rate, $\dot{\gamma}$, in 1/s.) The model parameters *a*, *b*, *c*, *d*, and *e* were solved by using MATLAB's fminsearch function (MathWorks; Natick, MA, USA). As viscosity values varied almost two orders of magnitude, a logarithm was taken of the measured and modeled viscosities before calculating the sum of the squares. The obtained model parameters were (R^2 = 0.99):

$$a = 17.3,\ b = 7.92,\ c = 0.459,\ d = 0.204,\ e = -2.15 \quad (14)$$

Figure 9 shows the modelled viscosity as a function of the measured viscosity. We see that the model works very well. We can define the relative deviation, δ_i, of the model prediction from the measured value for trial point *i* as:

$$\delta_i = \frac{\mu_i^{\text{model}} - \mu_i^{\text{exp}}}{\mu_i^{\text{exp}}} \quad (15)$$

For the whole data set, the standard deviation of δ_i was 9.5%, and $|\delta_i|$ was always smaller than 0.25.

Analysis of slip flow data

Figure 10 shows the entire measured slip data as a function of wall shear stress. The air content is shown with colors, and the viscosity of the PVOH solution is shown with the marker type. The inset figure shows the bubble size with colors. We see from Fig. 10 that the slip flow increases nonlinearly with increasing wall shear stress. We also see that slip flow generally decreases with increasing air content, increasing PVOH solution viscosity and decreasing bubble size. This observation can be explained as follows [16,17]: The slip layer is a pure fluid layer, and the slip effect increases with the increasing thickness of the layer. With higher PVOH concentration, the viscosity of the fluid layer is higher, and the slip effect is thus smaller. With higher air content and smaller bubbles (and subsequent thinner lamellae and smaller plateau borders), it is more difficult to drain fluid from the foam into the vicinity of the wall.

The (v_s; τ_w, μ_s, φ, *D*) data set was first studied to find out which quantities had a clear effect on the slip velocity. It was found that all four parameters had a statistically significant effect. It was also found that a power law also worked well here, i.e., the obtained model for slip was:

$$v_s = a\tau_w^b \mu_s^c \varphi^d D^e \quad (16)$$

(Notice that in Eq. 16, wall shear stress τ_w was expressed in Pa, PVOH solution viscosity μ_s in mPas, and bubble size *D* in μm.) The model parameters were obtained with a similar procedure as for the foam viscosity. The result was (R^2 = 0.99):

$$a = 3.18\text{e-}07,\ b = 1.60,\ c = -0.970,\ d = -6.89,\ e = 1.31 \quad (17)$$

The standard deviation of δ_i (see Eq. 15) was 11%, and $|\delta_i|$ was smaller than 0.25 for 96% of the trial points. **Figure 11** shows the modeled viscosity as a function of the measured viscosity. We see that while the model gener-

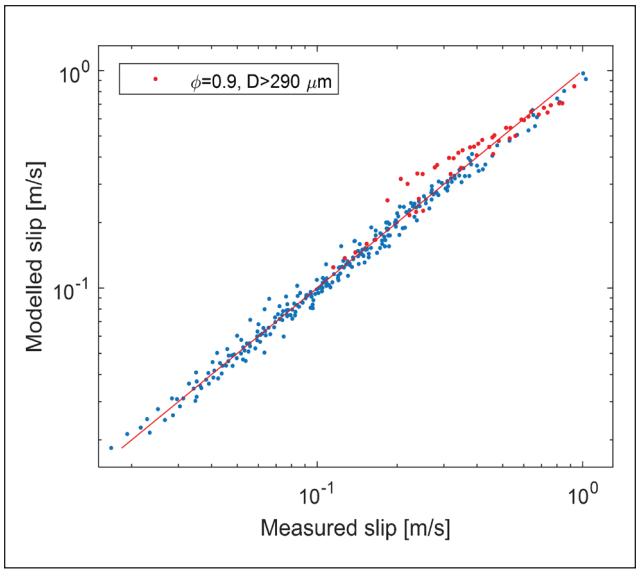

11. The modeled slip flow, Eq. 16, with the parameters of Eq. 17 as a function of the measured slip. There is a small subset of data points that deviate from the general trend. For these points, air content was 0.9 and bubble size was higher than 290 µm. The red line shows the curve **y = x**. *Coefficient of determination is* $R^2 = 0.99$.

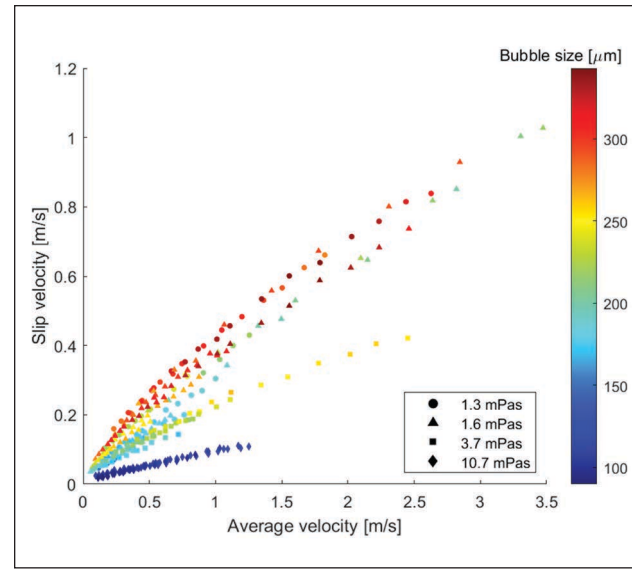

12. Slip velocity as a function of average flow velocity. The viscosity of the PVOH solution is shown with markers and the bubble size is shown with colors.

ally works very well, there is a small subset of data points that deviate slightly from the general trend. For these points, air content was 0.9 and bubble size was higher than 290 µm.

We also studied an alternate model for slip flow where the wall shear stress was replaced with the average flow velocity v_{avg} (**Fig. 12**). In this case, the obtained model was:

$$v_s = a v_{\text{avg}}^b \mu_s^c D^d \tag{18}$$

(In the preceding, flow velocity v_{avg} is expressed in m/s, PVOH solution viscosity in mPas, and bubble size in µm.) The model parameters given by the regression analysis were ($R^2 = 0.99$):

$$a = 0.00816,\ b = 0.733,\ c = -0.357,\ d = 0.704 \tag{19}$$

In this case, logarithm was taken before fitting on Eq. 18, and then the normal sum of the squares was used to find the model parameters.

Figure 13 shows the modeled slip flow Eq. 18, with the parameters of Eq. 19, as a function of the measured slip. We see that the model generally works very well. The standard deviation of δ_i (see Eq. 15) was 11%, and $|\delta_i|$ was smaller than 0.15 for 93% of the trial points.

Notice that for a slip model where bubble size was replaced with the air content in Eq. 18, the coefficient of determination was almost as high. However, including both these variables did not increase the coefficient of determination, and the least-angle regression (LARS) analysis suggested that, of the two quantities, the bubble size was preferred. Finally, notice that unlike Eq. 16, Eq. 18 cannot be used to calculate the slip velocity explicitly from the pressure loss, although the bubble size would be known.

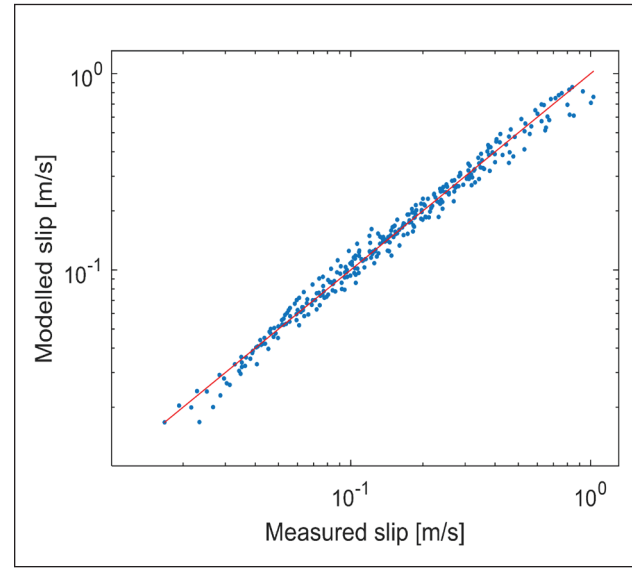

13. The modeled slip flow, Eq. 18, with the parameters of Eq. 19 as a function of measured slip. The red line shows the curve **y = x**. *Coefficient of determination is* $R^2 = 0.99$.

Earlier studies on foam rheology include: Princen and Kiss (1986) [10], Höhler and Cohen-Addad (2005) [11], Herzhaft et al. (2005) [12], Larmignat et al. (2008) [13], Heller and Kuntamukkula (1987) [23], Denkov et al. (2009) [24], Zhao et al. (2009) [25], and Soleymanzadeh et al. (2018) [26]. Unfortunately, we could not find any papers where PVOH foams would have been studied in de-

tail. Moreover, it is not easy to compare the obtained correlations for viscosity and slip, Eqs. 13 and 16, and their parameter values shown in Eqs. 14 and 17, with existing literature; as to our knowledge, no one has simultaneously varied both the air content and base solution viscosity in such a broad range and simultaneously measured the bubble size of the foam. The comparison in many cases necessitates gathering the comparison data from the figures, because functional forms may not have been given. Moreover, the used functional forms may differ from the ones we have chosen. As an example, Thondavadi and Lemlich [16] studied the flow of an aqueous foam made with a cationic surfactant in acrylic pipes, with air content varying from 0.88 to 0.99 and bubble size varying from 0.1 to 1 mm. We used a Matlab graphical interface for acquiring the slip flow-shear rate data from the figures and found that the exponent of wall shear stress (see Eq. 16) was identical (b = 1.6).

Thondavadi and Lemlich also studied flow in galvanized steel pipes. In that case, they did not observe slip flow at the pipe walls. In our test, we did not see a difference in the slip behavior of an acrylic pipe and a steel pipe (Material No. EN 1.4404). The reason behind the different results is likely that the roughness of the steel pipes used by Thondavadi and Lemlich was clearly higher.

CONCLUSIONS

The foam-assisted application process is a promising emerging technology for applying chemicals and dispersions into a wet web of paper or board. Development and upscaling of this novel technology necessitate a good understanding of the complex rheological behavior of foams used in the process.

In this study, we studied application foams made of PVOH, as it is already used in the industry as a strength additive. Foam density was varied between 100 g/L and 300 g/L, and the concentration of the PVOH solution was between 0.5% and 6.0%. The foams were generated with a commercial foam generator, and the rheological properties of the foams were measured with the flow of the foam in horizontal pipes. The viscosity and the dynamic surface tension of the PVOH solutions were quantified with commercial laboratory devices.

The analysis of viscosity results indicated that PVOH foams can be described with high accuracy as shear-thinning power law fluids where the detailed behavior depends on the foam density and the PVOH concentration. Slip flow, as usual, increased with increasing wall shear stress, but was also dependent on the PVOH concentration, the air content, and the bubble size. For both the foam viscosity and the slip flow, a correlation was found that described

ABOUT THE AUTHORS

We studied this topic because our industrial partners are developing foam-assisted application of additives onto a wet web. In this study, we have considerable variation in the main quantities affecting the foam rheology (air content, solution viscosity, and bubble size). The rheological models obtained are thus applicable for a wide range of foams.

This study's most difficult aspect was that the contribution of the slip flow on flow rate can be significant for foams, and slip should thus be measured accurately. We measured the slip flow explicitly by using transparent pipes and high-speed imaging.

In the literature, it is often claimed that there is no slip flow in steel pipes. Interestingly, we found that the slip in acrylic and steel pipes is similar if the roughness of the steel pipe is relatively low.

For mills, the foam-assisted application process is a promising emerging technology for applying chemicals and dispersions onto a wet web of paper or board. Despite the complex rheology of foams, the obtained models could be used to describe their behavior with a good accuracy. Development and upscaling of this technology necessitate a good understanding of the foam rheology. As a next step, a study of how the foam rheology depends on the absolute pressure level of the foams should be pursued.

Jäsberg is senior scientist, Viitala is research scientist, Tanaka is senior scientist, Prakash is senior scientist, and Koponen is principal scientist at VTT Technical Research Center of Finland Ltd. in Jyväskylä, Finland. Email Koponen at Antti.Koponen@vtt.fi.


Jäsberg

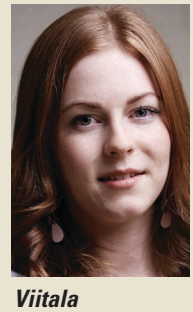
Viitala


Tanaka


Prakash


Koponen

the quantitative behavior of all the studied foams with good accuracy.

In the future, this work will be expanded for other surfactants and various surfactant-chemical/dispersion combinations relevant to the real foam application processes. Early results of this work indicate that correlations Eq. 13 and Eq. 16 with the values of exponents shown in Eq. 14 and Eq. 17 might not be PVOH specific. If this is the case, the properties of the real process foams could be determined at a mill by a small set of experiments, and the tedious work described in this study would be greatly simplified. **TJ**

ACKNOWLEDGMENTS

This research was done in the ChemFunc project funded in part by Business Finland. The authors want to thank ChemFunc project parties Metsä Board, Valmet, Solenis, Sulzer, Anpap, and Pixact for valuable discussion on this work and its results.

LITERATURE CITED

1. Sen, A.K., *Coated Textiles: Principles and Applications*, 2nd edn., CRC Press, Boca Raton, 2007.
2. Kenttä, E., Kumar, V., Andersson, P., et al., *AUTEX Res. J.* 22(3): 335(2022). https://doi.org/10.2478/aut-2021-0031.
3. Kinnunen-Raudaskoski, K., Hjelt, T., Kenttä, E., et al., *TAPPI J.* 13(7): 9(2014). https://doi.org/10.32964/TJ13.7.9.
4. Kenttä, E., Kinnunen-Raudaskoski, K., and Hjelt, T., *TAPPI J.* 13(7): 21(2014). https://doi.org/10.32964/TJ13.7.9.
5. Kinnunen-Raudaskoski, K., Salminen, K., Lehmonen, J., et al., *TAPPI J.* 15(11): 731(2016). https://doi.org/10.32964/TJ15.11.731.
6. Bliss, T., Luo, M., and Nicholas, M., *TAPPI J.* 20(1): 9(2021). https://doi.org/10.32964/TJ20.1.9.
7. Oksanen, A., Hjelt, T., Lehmonen, J., et al., *PaperCon,* TAPPI Press, Peachtree Corners, GA, USA, 2022.
8. Hjelt, T., Henriksson, E., Jaiswal, A.K., et al., *PaperCon*, TAPPI Press, Peachtree Corners, GA, USA, 2022.
9. Skelton, J., *Pap. Technol. Ind.*, 1987, pp. 431-436.
10. Princen, H.M. and Kiss, A.D., *J. Colloid Interface Sci.* 112(2): 427(1986). https://doi.org/10.1016/0021-9797(86)90111-6.
11. Höhler, R. and Cohen-Addad, S., *J. Phys.: Condens. Matter* 17: R1041(2005). https://doi.org/10.1088/0953-8984/17/41/R01.
12. Herzhaft, B., Kakadjian, S., and Moan, M., *Colloids Surf., A* 263(1-3): 153(2005). https://doi.org/10.1016/j.colsurfa.2005.01.012.
13. Larmignat, S., Vanderpool, D., Lai, H.K., et al., *Colloids Surf., A* 322(1-3): 199(2008). https://doi.org/10.1016/j.colsurfa.2008.03.010.
14. Jäsberg, A., Selenius, P., and Koponen, A., *Colloids Surf., A* 473: 147(2015). https://doi.org/10.1016/j.colsurfa.2014.11.041.
15. Koponen, A., Eloranta, H., Jäsberg, A., et al., *TAPPI J.* 18(8): 487(2019). https://doi.org/10.32964/TJ18.8.487.
16. Thondavadi, N.N. and Lemlich, R., *Ind. Eng. Chem. Process Des. Dev.* 24(3): 748(1985). https://doi.org/10.1021/i200030a038.
17. Gardiner, B.S., Dlugogorski, B.Z., and Jameson., G.J., *Ind. Eng. Chem. Res.* 38(3): 1099(1999). https://doi.org/10.1021/ie980385i.
18. Barnes, H.A., *J. Non-Newtonian Fluid Mech.* 56(3): 221(1988). https://doi.org/10.1016/0377-0257(94)01282-M.
19. Gottberg, J.M., Lappalainen, T., and Salminen, K., *TAPPI J.* 18(8): 475(2019). https://doi.org/10.32964/TJ18.8.475.
20. Takasu, A., Ohmori, S., Yamauchi, Y., et al., *J. Polym. Sci., Part A: Polym. Chem.* 40(24): 4477(2002). https://doi.org/10.1002/pola.10538.
21. Mooney, M., *J. Rheol.* 2: 210(1931). https://doi.org/10.1122/1.2116364.
22. Morrison, F.A., *Understanding Rheology,* Oxford University Press, New York, 2001.
23. Heller, J. and Kuntamukkula, M., *Ind. Eng. Chem. Res.* 26(2): 318(1987). https://doi.org/10.1021/ie00062a023.
24. Denkov, N.D., Tcholakova, S., Golemanov, K., et al., *Soft Matter* 5: 3389(2009). https://doi.org/10.1039/B903586A.
25. Zhao, J., Pillai, S., and Pilon, L., *Colloids Surf., A* 348(1-3): 93(2009). https://doi.org/10.1016/j.colsurfa.2009.06.037.
26. Soleymanzadeh, A., Gahrooei, H.R.E., and Joekar-Niasar, V., *J. Energy Resour. Technol.* 140(3): 032911(2018). https://doi.org/10.1115/1.4038385.

ABOUT THIS PAPER

Cite this article as:
Jäsberg, A., Viitala, J., Tanaka, A., et al., *TAPPI J.* 22(1): 51(2023). https://doi.org/10.32964/TJ22.1.51

DOI: https://doi.org/10.32964/TJ22.1.51

ISSN: 0734-1415

Publisher: TAPPI Press

About this journal